Storage of a spectrally shaped hologram in a frequency selective material



1995 J. Phys. B: At. Mol. Opt. Phys. 28 L565

(http://iopscience.iop.org/0953-4075/28/17/008)

J. Phys. B: At. Mol. Opt. Phys. 28 (1995) L565–L570. Printed in the UK

LETTER TO THE EDITOR

# Storage of a spectrally shaped hologram in a frequency selective material

I Lorgeré†, M Rätsep†‡, J-L Le Gouët†, F Grelet†, M Tian†§, A Débarre† and P Tchénio†

† Laboratoire Aimé Cotton, CNRS II Bât. 505, Campus d'Orsay, 91405 Orsay Cédex, France
‡ Institute of Physics, Estonian Academy of Sciences, EE2400 Tartu, Estonia
§ Changchun Institute of Physics, Chinese Academy of Sciences, People's Republic of China

Received 18 April 1995

**Abstract.** A spectral holography experiment is performed in a hole-burning material. A shaping device is used to tailor the spectrum of the pulses which engrave the hologram. The resolution of the spectral shaping technique is investigated both theoretically and experimentally.

Linear spectral filtering has proved to be a powerful technique for temporal shaping of ultrashort light pulses [1–7]. The technique consists of spatially dispersing the frequency components of a short pulse in order to filter the components through phase and amplitude masks. Recombination of the filtered components then gives the desired temporal shape. The technique has been used to synthesize femtosecond waveforms according to specifications in experiments involving all-optical switching [6], dark soliton propagation in fibres [4] and pulse coding for communication [5].

Recently Weiner *et al* demonstrated a spectral holography technique which allows the recording and non-linear filtering of temporal waveforms [7]. A hologram is recorded as a spatial interference pattern on a conventional holographic plate placed in the filtering plane of a pulse shaper. Time-reversal, convolution and correlation of femtosecond waveforms have been demonstrated with this technique. Spectral holography can also be performed in a frequency selective recording material through the processes of time-delayed DFWM and spectral hole-burning [8–10]. For recording, the hole-burning material is illuminated by two pulses separated by the time delay $T$. One is a short pulse that serves as a time-domain reference. The other is the temporally structured object pulse. Thus the spectral interference pattern between the object and the reference pulses is stored as a modification of the inhomogeneously broadened absorption band of the material. The engraved spectral pattern is the spectral hologram. Subsequent excitation of the material by a short reading pulse gives rise to emission of a signal after a delay equal to $T$. The shape of the emitted signal is that of the recorded object pulse or its time-reversed version depending on the time order of the object and the reference pulses. With a temporally structured reading pulse the emitted signal waveform is the result of the convolution or the correlation of the reading and the object temporal shapes [11]. The development of spectral holography in hole-burning materials is limited by the necessary cryogenic technique. In addition the excitation spectrum must match the absorption band of the material. On the other hand, hole-burning materials make it possible to record and process both spectral and spatial

0953-4075/95/170565+06$19.50  

structures which is not the case with the above holographic technique [7]. For this reason hole-burning materials are attractive for high-density image storage and parallel processing [12–15].

Pulse shapers may prove useful in the development of hole-burning memories and processors. A spectral encoding technique using a pulse shaper has recently been proposed for addressing images stored as spectral holograms [16]. The development of such techniques is conditioned by their spectral resolution, that is, by the width of the smallest spectral feature that can be processed in the experiment. The spectral resolution of a pulse shaper was studied both theoretically and experimentally [2]. It was found that this resolution was limited by the size of the diffraction spot produced by the input beam on the filtering plane. This letter shows theoretically that a resolution below this limit can be obtained with a pulse shaper. A spectral holography experiment in a hole-burning material is reported which demonstrates the theoretical conclusions.

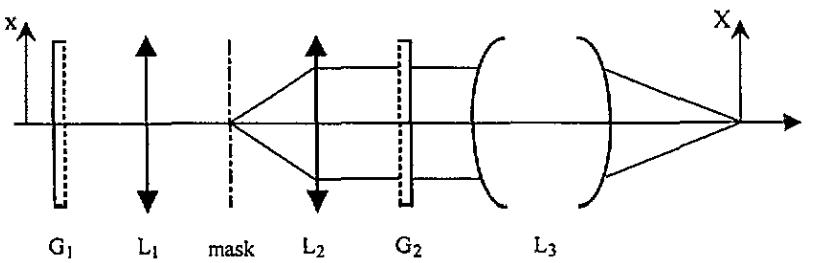


**Figure 1.** Sketch of the optical system. The grating pair $G_1$ and $G_2$ together with the mask and the lenses $L_1$ and $L_2$ form the pulse shaper. The lens $L_2$ together with the optical combination $L_3$ form an imaging system that conjugates the mask and the $X$-plane.

Let us consider the optical system sketched in figure 1. It consists of a pulse shaper followed by an optical combination that focuses the beam on a plane ($X$-plane), where the shaped pulses are observed. The pulse shaper device is that first proposed by Froehly and further developed by Weiner *et al* [1, 7]. It is made of a unit magnification telescope with a pair of gratings placed in its outer focal planes. The spectrum of the input pulse spreads in the plane situated midway between the lenses. Phase and amplitude masks placed in this plane filter the spectral components of the pulse. These components are recombined together by the output lens and grating, symmetric with the input dispersing system. The output lens of the telescope together with the combination $L_3$ form an imaging system that conjugate the mask and the $X$-plane. The pulse entering the shaper is described by the spectral amplitude $E_i(x;\omega) = E(\omega)E_i(x)$ of the optical field. The variable $\omega$ is the frequency shift with respect to the central frequency $\Omega_0$ of the pulse spectrum. The function $E_i(x)$ gives the beam shape in the grating plane of incidence. The beam shape in the perpendicular direction is not considered since it is not affected by the gratings. The action of the gratings on the above field is described following Martinez [17]. The relevant parameters are the angular dispersion coefficient $\beta = -\partial\theta/\partial\omega$ of the gratings and the coefficient $\alpha = -\partial\theta/\partial\gamma$ which gives the relative variations of the diffraction angle and of the incident angle on the first grating (i.e. the angular magnification of the first grating). Accounting for the gratings, and describing the propagation of the pulse through the optical system with the diffraction theory, one finds that the field $E(X;\omega)$ on the $X$-plane is expressed as

$$E(X;\omega) = E(\omega)\int du\, m(u)\hat{E}_i\left(\frac{u-\beta f\omega}{\alpha\lambda f}\right)R(u-\beta f\omega+\alpha X/g) \qquad (1)$$

where $\lambda = 2\pi c/\Omega_0$, $f$ is the focal length of the telescope and $g$ is the transverse magnification of the imaging system. The function $\hat{E}_i(\xi) = \int dx\, E_i(x) \exp 2i\pi x\xi$ is the spatial Fourier transform of the input field $E_i(x)$. It describes the diffraction spot produced by the input beam on the mask (for one frequency component). The function $R(u)$ is the impulse response function of the reversed imaging system, accounting for its apertures: it describes the diffraction spot that the imaging system would produce on the mask in response to a point source located on the $X$-plane (if the light direction of propagation were reversed). The mask is represented by the function $m(u)$. The integral is the effective spectral mask as seen by the point $X$ on the observation plane. It is the convolution of the physical mask with the product of the impulse response and of the input beam diffraction spot. This means that the spectral resolution of the device is determined by the width of the input beam diffraction spot or by that of the impulse response, depending on which is the smallest. The size of the input beam diffraction spot depends mostly upon the transverse coherence length of the beam. In an experimental situation it is rather difficult to achieve a large spatially coherent beam and therefore a small diffraction spot. On the other hand, the impulse response width only depends upon the apertures of the imaging system and can be made very small. As a result the spectral resolution of the system is in practice determined by the impulse response width and is independent of the input beam coherence length. It follows that in order to produce a faithful spectral image of the physical mask in the spectrum $E(X;\omega)$, it is only required that the impulse response width be much smaller than the size $d$ of the smallest mask feature. In our device, the aperture of the imaging system has an $O = 25$ mm diameter and lies in the plane of the telescope output grating. The above condition therefore gives $d \gg \lambda f/O = 6\ \mu$m ($f = 250$ mm). With 1800 grooves/mm gratings giving a 2500 rad nm$^{-1}$ angular dispersion and a typical 5 nm input bandwidth, this allows the synthesis of spectral patterns with several hundred independent features. Under the above condition the field in the $X$-plane reads as

$$E(X;\omega) = E(\omega)\hat{E}_i(-X/g\lambda f)m(\beta f\omega - \alpha X/g)\,. \tag{2}$$

In this expression the spectral mask depends upon the position in the $X$-plane. But this dependence is a mere shift in frequency. At every point of the $X$-plane, the shape of the spectral mask is that of the physical mask whatever the input beam shape. The frequency shift can be understood with geometrical optics considerations. Let us consider the frequency component $\omega$ of the pulse. This component is focused on the mask around the point $u = \beta f\omega$. It spreads over an area whose typical size $w_0$ is the input beam diffraction spot width. The image of this spot on the $X$-plane spreads over an area of width $w_0 g/\alpha$ centred on the point $X = 0$. The central point of the $X$-plane is the image of the central point of the spot on the mask. For this point the filtering mask is therefore $m(\beta f\omega)$. But at distance $X$ from the central point one observes the image of the point located at $u = \beta f\omega - \alpha X/g$ on the mask. Hence the point $X$ sees a shifted mask, as indicated by (2).

The above discussion assumes that the mask and the $X$-plane are perfectly conjugated by the imaging system. In an experimental situation it might not be easy to fulfil this condition. Failure to do so results in enlargement of the impulse response and deterioration of the spectral resolution. Let us consider a default $\varepsilon$ (conjugation default) between the position of the mask and the position of the $X$-plane conjugate. The angular aperture of the beam leaving the mask is $\lambda/d$. The image of a point of the sample on the mask therefore spreads over a spot of size $\varepsilon\lambda/d$. For the conjugation default not to spoil the spectral resolution of the system it is necessary that this geometrical spot be much smaller than the size $d$ of the smallest mask feature. This condition demands that the default $\varepsilon$ be much smaller than $d^2/\lambda$ that is $\sim$3.3 mm with $d = 45\ \mu$m. This means that in a practical situation

the conjugation default is the key parameter to achieving a good spectral resolution. If care is not taken in this parameter, one may reach the situation when the width of the impulse response is larger than the input beam diffraction spot, in which case the spectral resolution is determined by the input beam diffraction spot. This may explain the results found by Weiner in his early works on pulse shaping devices [2].

In order to check the validity of the above analysis we have performed a spectral holography experiment in a hole-burning material (octaethylporphine in polystyrene at 1.4 K). This experiment is related to our interest in the storage capabilities of such materials [18, 19, 16]. The experiment is the following. First the spectral structure of an object pulse which has been synthesized with the pulse shaper is recorded as a spectral hologram in the hole-burning material. Then the stored structure is probed by a test pulse which has also been structured by the pulse shaper and the energy of the holographic signal recorded.

The holographic signal is described by the amplitude $E_S(X;\omega)$ of the corresponding field on the sample. This amplitude can be expressed as

$$E_S(X;\omega) = E_1^*(X;\omega)E_2(X;\omega)E_3(X;\omega)\,. \tag{3}$$

In this expression, the field $E_2(X;\omega)$ describes the short unstructured pulse used as a reference for the holographic recording. The field $E_1(X;\omega)$ describes the object pulse whose spectral shape is stored in the sample while the field $E_3(X;\omega)$ is that of the reading pulse used to probe the hologram. The mask used to shape the object pulse is an amplitude mask which consists of ten transparent ~45 $\mu$m width slits separated from each other by the periodic distance $p = 400$ $\mu$m. The same mask is used for shaping the test pulse except that it is shifted by the distance $u_0$ with respect to the recording mask. The width of our imaging system impulse response is typically 6 $\mu$m. As a consequence it can be neglected at the scale of the mask slits. Therefore, if the sample is perfectly positioned with respect to the mask plane and the spectrum $E(\omega)$ is flat other the mask width, the energy $W(u_0) = \int \mathrm{d}X \int \mathrm{d}\omega |E_s(X;\omega)|^2$ of the holographic signal, recorded as a function of the mask shift $u_0$, is proportional to the autoconvolution function of the mask:

$$W(u_0) \propto \int \mathrm{d}\omega\, m(\beta f \omega) m(\beta f \omega - u_0)\,. \tag{4}$$

This function consists of $2d$-width triangles spaced by the distance $p$. The amplitude of the triangles decreases as the shift $u_0$ increases due to the finite width of the mask. It should be pointed out that (4) relies on the assumption that the sample is not translated in the $X$-direction between the recording and the reading steps. Translating the sample by the distance $X_0$ is equivalent to shifting the mask by $\alpha X_0/g$. This is not significant in this particular experiment because the whole convolution function $W(u_0)$ is recorded. But this feature should be considered in experiments such as the one proposed in [16], where the hole-burning material is used to process one specific point of the convolution function of the recording and the reading mask.

We have not tried to measure the spectral resolution limit of our device. Instead, we have measured the cross-talk between the spectral slices cut in the field spectrum by the mask slits. The cross-talk is defined by the ratio $W(u_0 = d)/W(0)$. It is the value of the signal energy in the wings of the triangle relative to the peak energy value. This parameter measures the independence of the spectral slices. It is related to the spectral resolution of the experiment. It approaches zero when the spectral resolution is much better than the spectral width of the mask slits.

Figure 2 shows experimental profiles of the signal energy $W(u_0)$. The first one (figure 2($a$)) gives the overall characteristics of the profiles. The irregular variation of the peak amplitudes is probably due to the fact that the spectral bandwidth (FWHM ~ 3 nm)

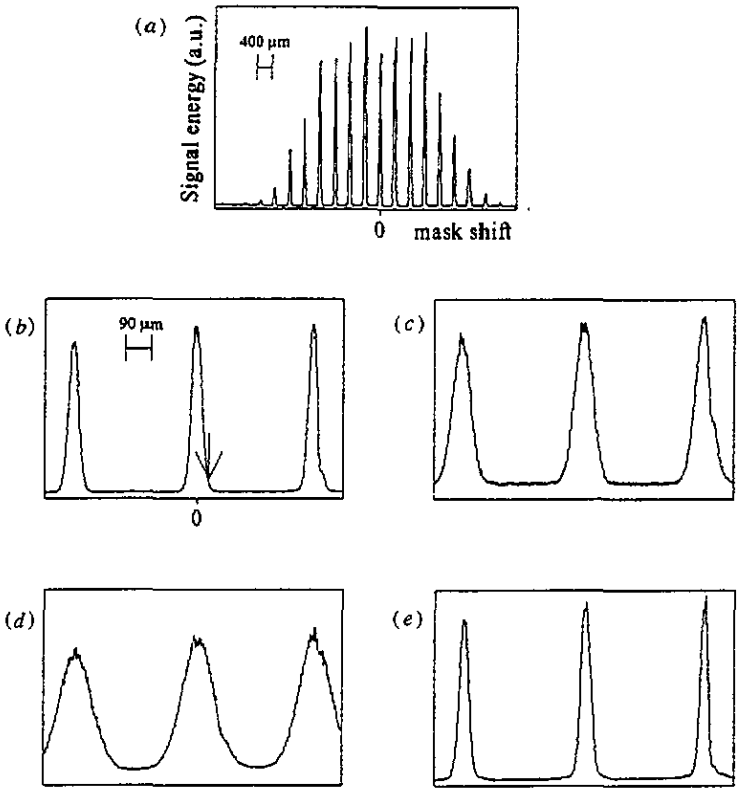


**Figure 2.** Experimental records of the holographic signal energy as a function of the shift $u_0$ between the recorded and the testing masks: (*a*) general aspect of the records, (*b*) first three central peaks recorded with optimal conditions (the arrow indicates where the cross-talk is measured), (*c*) with a 5 mm conjugation default, (*d*) with a 5 mm conjugation default and a 2 mm aperture on the input beam and (*e*) with a 2 mm aperture on the input beam but a zero conjugation default.

of the laser is not uniform over the mask width (5.8 nm). Figure 2(*b*) shows the first three central peaks recorded when the conjugation between the mask and the sample plane is optimally adjusted. This corresponds to optimal conditions to achieve good spectral resolution. This profile shows the triangular shape of the peaks. The cross-talk is best measured on the central peak because the others are affected by the irregularity of the mask pattern. The FWHM of this peak is 41 $\mu$m which is close to the expected value. The cross-talk value is 3.8%. Figure 2(*c*) shows the influence of the conjugation default. For the recording of this profile, the parameter $\varepsilon$ was set to 5 mm. This results in broadening of the peaks and an increase of the cross-talk. The FWHM of the central peak is 69 $\mu$m and the cross-talk value measured on this peak is 32%. With such a large conjugation default one would expect a larger cross-talk value. This indicates that the spectral resolution is actually determined by the width of the input beam diffraction spot as confirmed by figure 2(*d*). This profile was recorded with the same conjugation default, but in addition, the input beam was limited by a 2 mm diameter aperture on lens $L_1$. The result is a considerable increase of the peak width (125 $\mu$m) and of the cross-talk, the latter now reaching 70%. For the profile of figure 2(*e*), the same limiting aperture was used but the conjugation was best adjusted. The

FWHM of the peak (38 $\mu$m) is now again close to the theoretical value and the cross-talk value is only 3.4%. This shows that the spectral resolution is indeed independent of the input beam size provided that the sample is in the image plane of the mask.

In summary this letter demonstrates that the spectral resolution of a pulse shaper is independent of the input beam size when the shaped pulses are observed in the image plane of the shaping mask. The spectral resolution is then determined by the width of the imaging system impulse response. We have also demonstrated the storage and readout of a spectrally shaped hologram in a frequency selective material. These results are encouraging for the development of pulse shaping techniques in hole-burning memory devices.

## References


[1] Frœhly C, Colombeau B and Vampouille M 1983 Shaping and analysis of picosecond light pulses ed E Wolf *Progress in Optics XX* (Amsterdam: North-Holland) pp 65–153

[2] Thurston R N, Heritage J P, Weiner A M and Tomlinson W J 1986 Analysis of picosecond pulse shape synthesis by spectral masking in a grating pulse compressor *IEEE J. Quantum Electron.* **22** 682

[3] Weiner A M, Laird D E, Patel J S and Wullert J R 1992 Programmable shaping of femtosecond optical pulses by use of 128 element liquid crystal phase modulator *IEEE J. Quantum Electron.* **28** 908–19

[4] Weiner A M, Thurston R N, Tomlinson W J, Heritage J P, Laird D E, Kirshner E M and Hawkins R J 1989 Temporal and spectral self-shifts of dark optical solitons *Opt. Lett.* **14** 868

[5] Weiner A M, Heritage J P and Salehi J A 1988 Encoding and decoding of femtosecond pulses *Opt. Lett.* **13** 300

[6] Weiner A M, Silberberg Y, Foukhardt H, Laird D E, Saifi M A, Andrejco M J and Smith P V 1989 Use of femtosecond square pulses to avoid pulse breakup in all-optical switching *IEEE J. Quantum Electron.* **25** 2648

[7] Weiner A M, Laird D E, Reitze D H and Paek E G 1992 Spectral holography of shaped femtosecond pulses *Opt. Lett.* **17** 224

[8] Rebane A, Kaarli R and Saari P 1983 Photochemical time-domain holography of weak picosecond pulses *Opt. Commun.* **47** 173

[9] Saari P, Kaarli R and Rebane A 1986 Picosecond time and space domain holography by photochemical hole-burning *J. Opt. Soc. Am.* B **3** 527

[10] Kim M K and Kachru R 1987 Storage and phase conjugation of multiple images using backward-stimulated echoes in $Pr^{3+}$:$LaF_3$ *Opt. Commun.* **12** 593–5

[11] Bai Y S, Babitt W R, Carlson N W and Mossberg T W 1984 Real time optical waveform convolver/cross-correlator *Appl. Phys. Lett.* **45** 714–6

[12] Mitsunaga M, Yano R and Uesugi N 1991 Time and frequency domain hybrid optical memory: 1.6 Kbit data storage in $Eu^{3+}$:$Y_2SiO_5$ *Opt. Lett.* **16** 1890

[13] Shen X A and Kachru R 1993 Time-domain optical memory for image storage and high speed image processing *Appl. Opt.* **32** 5811

[14] Sasaki H and Karaki K 1994 Hole-burning holography in $Eu^{3+}$:$Y_2SiO_5$ *Persistent Spectral Hole-Burning and Related Spectroscopies: Science and Applications* (Optical Society of America) p 384

[15] Kohler B, Bernet S, Renn A and Wild U P 1991 Holographic optical data storage of 2000 images by photochemical hole-burning *Persistent Spectral Hole-Burning: Science and Application* (Optical Society of America) pp 46–9

[16] Sõnajalg H, Débarre A, Le Gouët J-L, Lorgeré I and Tchénio P 1995 Phase encoding technique in time-domain holography: theoretical estimation *J. Opt. Soc. Am.* B accepted

[17] Martinez O E 1986 Grating and prism compressors in the case of finite beam size *J. Opt. Soc. Am.* B **3** 929

[18] Débarre A, Keller J-C, Le Gouët J-L and Tchénio P 1991 Field cross-correlation retrieval of optically stored data *J. Opt. Soc. Am.* B **8** 153–9

[19] Débarre A, Keller J-C, Le Gouët J-L, Tchénio P and Galaup J-P 1991 Optical information storage in condensed matter with stochastic excitation *J. Opt. Soc. Am.* B **12** 2529–36